Letter

Observation of the singly Cabibbo-suppressed decay $\Lambda_c^+ \to \Sigma^- K^+ \pi^+$

M. Ablikim *et al.*[*]
(BESIII Collaboration)

(Received 12 September 2023; revised 6 November 2023; accepted 2 April 2024; published 30 April 2024; corrected 23 May 2024)

The singly Cabibbo-suppressed decay $\Lambda_c^+ \to \Sigma^- K^+ \pi^+$ is observed for the first time with a statistical significance of 5.4σ by using 4.5 fb^{-1} of e^+e^- collision data collected at center-of-mass energies between 4.600 and 4.699 GeV with the BESIII detector at BEPCII. The absolute branching fraction of $\Lambda_c^+ \to \Sigma^- K^+ \pi^+$ is measured to be $(3.8 \pm 1.2_{\mathrm{stat}} \pm 0.2_{\mathrm{syst}}) \times 10^{-4}$ in a model-independent approach. This is the first observation of a Cabibbo-suppressed Λ_c^+ decay involving Σ^- in the final state. The ratio of branching fractions between $\Lambda_c^+ \to \Sigma^- K^+ \pi^+$ and the Cabibbo-favored decay $\Lambda_c^+ \to \Sigma^- \pi^+ \pi^+$ is observed to be $(0.4 \pm 0.1)s_c^2$, where $s_c \equiv \sin\theta_c = 0.2248$ with θ_c the Cabibbo mixing angle.

DOI: 10.1103/PhysRevD.109.L071103

Understanding the nonfactorization contribution is critically challenging for advancing our knowledge of the hadronic weak decays of charmed baryons, as W exchange and inner W emission are no longer subject to helicity and color suppression [1]. The evaluation of nonfactorizable terms is far more difficult than that of factorizable ones and thus the constraints with experimental results are essential. Studies on the charmed baryon decays in experiment have promoted the understanding on the mechanism of charmed baryon decays. Nevertheless, there are still some puzzles needed to be understood. For example, why does the breaking effects arising from $m_s \gg m_{u,d}$ under SU(3) flavor symmetry significantly exist in the decays of Ξ_c^0 [2], but much smaller in Λ_c^+ decays [3,4]? Furthermore, the discrepancy between the experimental results and the theoretical prediction for the branching fraction (BF) of the decay $\Lambda_c^+ \to p\pi^0$ may indicate the significant contribution of a nonfactorization component and the interference between nonfactorization and factorization contributions [5–7]. Therefore, correctly estimating the nonfactorization contribution is still one of core tasks in the charm baryon physics.

Extensive studies on Cabibbo suppressed (CS) decays of charmed baryon in both experiment and theory have been conducted for two-body decays [8,9], because both the factorization and nonfactorization contributions are involved. But the majority of them could not be well described by phenomenological models [5–7,10–15]. This indicates the current description of the nonfactorization contribution is still not fully reliable. More experimental information is desirable, especially for the decays with hyperons, because the experimental results of CS processes with a hyperon in the final state are still limited. Until now, data for three-body CS decays exist only for the Σ^+. The decay $\Lambda_c^+ \to \Sigma^- K^+ \pi^+$ is the simplest singly CS process with a Σ^- directly in the final state, where the W-exchange and inner W-emission diagrams are expected to play the dominant role, as shown in Fig. 1. Therefore, the observation of the CS process $\Lambda_c^+ \to \Sigma^- K^+ \pi^+$ and the comparison with the Cabbibo favored (CF) decay $\Lambda_c^+ \to \Sigma^- \pi^+ \pi^+$ will open a new window for probing $\mathrm{SU(3)}_F$ breaking effects and the nonfactorization contribution in Λ_c^+ decays.

According to recent constraints provided by the reported branching fraction of the inclusive decay $\Lambda_c^+ \to n + X$ [16], there is large room to probe experimentally for decays with a neutron in the final state, including the Λ_c^+ decays to Σ^-, as $\Sigma^- \to n\pi^-$ almost saturates the branching fraction. At present, two-body CS processes involving the lighter baryons (p [17,18], n [10], Λ [4,19]) or $\Sigma^{+/0}$ hyperon [19,20] from Λ_c^+ decays have already been confirmed and

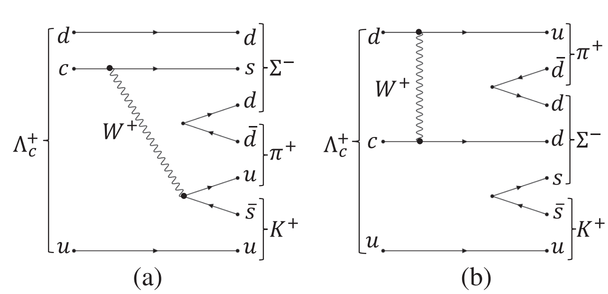

FIG. 1. Feynman diagrams for the CS decay $\Lambda_c^+ \to \Sigma^- K^+ \pi^+$: (a) internal W emission, (b) W exchange.

[*]Full author list given at end of the article.

studied extensively in experiment. However, no CS decays with a Σ^- have been observed.

Processes with Σ^- can be investigated by reconstructing the neutron signal through its missing energy under energy-momentum conservation at BESIII. Starting from threshold for Λ_c^+ pair production at 4.600 GeV, in this Letter, the first observation of the singly CS decay $\Lambda_c^+ \to \Sigma^- K^+ \pi^+$ is reported using 4.5 fb^{-1} of e^+e^- collision data collected with the BESIII detector at seven center-of-mass (c.m.) energies between 4.600 and 4.699 GeV [21]. Throughout this Letter, charge-conjugate modes are implicitly included.

Details about the design and performance of the BESIII detector can be found in Ref. [22]. Simulated samples are produced with a Geant4-based [23] Monte Carlo (MC) toolkit, which includes the geometric description [24] of the BESIII detector. Signal MC samples of $e^+e^- \to \Lambda_c^+\bar{\Lambda}_c^-$ with $\bar{\Lambda}_c^-$ decaying into ten hadronic modes and Λ_c^+ to $\Sigma^- K^+ \pi^+$, $\Xi^- K^+ \pi^+$, and $\Xi^{*0} K^+$ are used to determine the detection efficiencies, where the intermediate states are required to be $\Sigma^- \to n\pi^-$ and $\Xi^{*0} \to \Xi^- \pi^+$ with Ξ^- subsequently decaying through any allowed process. The ten hadronic decay modes are presented in Table I. These samples are generated for the individual c.m. energy by the generator KKMC [25] incorporating initial-state radiation effects and the beam-energy spread. The inclusive MC samples, consisting of open-charm states, radiative return to charmonium (like) ψ states, and continuum processes $e^+e^- \to q\bar{q}$ ($q = u, d, s$), are generated to survey potential backgrounds. Particle decays are modeled with EvtGen [26,27] using BFs taken from the Particle Data Group [3], when available, or otherwise estimated with LUNDCHARM [28,29]. Final-state radiation from charged final-state particles is incorporated using PHOTOS [30].

The double-tag (DT) approach is employed to measure the absolute branching fraction of $\Lambda_c^+ \to \Sigma^- K^+ \pi^+$. A data sample of $\bar{\Lambda}_c^-$ baryons, referred to as the single-tag (ST) sample, is reconstructed with ten exclusive hadronic decay modes, as the aforementioned and listed in Table I. The procedure of selecting the ST $\bar{\Lambda}_c^-$ baryon decays is described in Refs. [10,31,32], where 105249 ± 386 ST events are reconstructed in data. The fit curves for the beam-constrained mass M_{BC} of ST modes and their yields are summarized in Supplemental Material [33]. Those events in which the signal decay $\Lambda_c^+ \to \Sigma^- K^+ \pi^+$ is reconstructed in the system recoiling against the $\bar{\Lambda}_c^-$ candidates of the ST sample are denoted as DT candidates.

The decay $\Lambda_c^+ \to \Sigma^- K^+ \pi^+$ with $\Sigma^- \to n\pi^-$ is searched for among the remaining tracks recoiling against the ST $\bar{\Lambda}_c^-$ candidates. Particle identification (PID) is implemented by combining measurements of the ionization energy loss in the helium-based multilayer drift chamber (MDC) ($\mathrm{d}E/\mathrm{d}x$) and the flight time in the time-of-flight system. Only three charged tracks, detected in the MDC and reconstructed within a polar angle (θ) range of $|\cos\theta| < 0.93$, set by the drift chamber acceptance, are allowed for a DT signal candidate event, where θ is defined with respect to the z axis, which is the symmetry axis of the MDC. Two of the charged tracks, whose distances of closest approach to the interaction point (IP) must be less than 10 cm along the z axis ($|V_z| < 10$ cm) and less than 1 cm in the transverse plane ($|V_r| < 1$ cm), are assigned to be K^+ and π^+, according to the PID probability. A vertex fit is performed to the K^+ and π^+ candidates, and the momenta updated by the fit are used in the subsequent analysis. A third track, identified as a π^-, is assigned to originate from the Σ^- decay if its distance of the closest approach to the IP is within ± 20 cm along the z axis ($|V_z| < 20$ cm). To suppress background events containing other long-lived particles in the final state, the candidate events are further required to have no extra charged tracks with $|\cos\theta| < 0.93$, $|V_r| < 1$ cm, and $|V_z| < 20$ cm.

The neutron signal could be observed in $M_{\mathrm{rec}}(B^0)$, where the recoiling mass $M_{\mathrm{rec}}(B^0)$ is calculated as

$$[M_{\mathrm{rec}}(B^0)]^2 = \left[E_{\mathrm{beam}} - \sum\nolimits_i E_i\right]^2 \Big/ c^4 - \left|\rho \cdot \vec{p}_0 - \sum\nolimits_i \vec{p}_i\right|^2 \Big/ c^2. \quad (1)$$

TABLE I. The DT detection efficiencies (%) for $\Lambda_c^+ \to \Sigma^- K^+ \pi^+ / \Lambda_c^+ \to \Xi^- K^+ \pi^+ / \Lambda_c^+ \to \Xi(1530)^0 K^+$ for each ST mode at c.m. energies between $\sqrt{s} = 4.600$ and 4.699 GeV.

Channel/$\sqrt{s}$ (GeV)	4.600	4.612	4.628	4.641	4.661	4.682	4.699
$\bar{p}K^+\pi^-$	16.5/8.5/8.2	15.6/8.0/7.8	15.1/7.7/7.6	15.0/7.7/7.7	14.8/7.4/7.6	14.1/7.4/7.3	14.0/7.2/7.3
$\bar{p}K_S^0$	18.7/9.7/9.7	17.5/9.0/9.1	16.9/8.5/8.2	16.5/8.5/8.6	15.7/8.3/8.3	15.7/8.0/8.1	15.1/7.8/7.9
$\bar{p}K^+\pi^-\pi^0$	4.6/1.9/1.9	4.2/2.3/2.0	4.1/2.2/2.0	4.4/2.2/1.8	3.9/2.1/1.7	4.3/1.9/1.6	4.2/2.1/1.7
$\bar{p}K_S^0\pi^0$	6.5/3.3/3.3	6.0/3.0/2.8	5.2/2.7/2.6	5.3/2.9/2.8	5.2/2.8/2.7	5.3/2.8/2.6	5.2/2.6/2.5
$\bar{p}K_S^0\pi^+\pi^-$	6.2/3.1/3.1	5.5/2.8/2.8	5.2/2.8/2.6	5.5/2.7/2.7	5.2/2.9/2.9	5.0/2.6/2.6	4.9/2.6/2.5
$\bar{\Lambda}\pi^-$	14.5/7.1/7.1	12.7/7.1/7.2	12.3/6.4/6.6	12.1/6.5/6.7	12.5/6.0/6.0	11.0/6.1/6.0	11.7/5.4/5.5
$\bar{\Lambda}\pi^-\pi^0$	5.7/2.8/2.8	5.1/2.5/2.5	4.7/2.4/2.4	4.7/2.4/2.4	4.7/2.3/1.8	4.5/2.3/1.6	4.3/2.1/1.8
$\bar{\Lambda}\pi^+\pi^-\pi^-$	4.0/1.9/1.9	3.6/1.9/1.8	3.7/1.7/1.7	3.6/1.7/1.6	3.3/1.9/1.8	3.6/1.8/1.6	3.6/1.8/1.8
$\bar{\Sigma}^0\pi^-$	8.2/4.0/4.0	7.3/3.7/3.6	6.4/3.2/3.1	7.1/3.3/3.1	6.8/3.1/3.2	6.8/3.1/3.2	6.0/2.9/2.7
$\bar{\Sigma}^-\pi^+\pi^-$	6.6/3.3/3.3	6.3/3.1/3.0	6.1/3.1/3.0	5.4/2.8/2.9	5.5/2.9/2.6	5.5/2.7/2.6	5.5/2.6/2.6

Here E_i and $\vec{p}_i$ represent the energy and momentum, respectively, of particle i (K^+, π^+, or π^-), $\rho = \sqrt{E^2_{\rm beam}/c^2 - m^2_{\Lambda_c^+}c^2}$, and $\hat{p}_0 = -\vec{p}_{\bar{\Lambda}_c^-}/|\vec{p}_{\bar{\Lambda}_c^-}|$ is the unit direction opposite to the ST $\bar{\Lambda}_c^-$, where $m_{\Lambda_c^+}$ is the known Λ_c^+ mass [3]. The Σ^- signal reconstructed through $M_{\rm rec}(H^-)$, which is as defined in Eq. (1), with the subscript i now representing the K^+ and π^+ particles. To suppress the continuum hadron background (denoted as $q\bar{q}$ hereafter), the recoiling mass against the ST $\bar{\Lambda}_c^-$ in the center-of-mass frame, defined as

$$M_{\rm rec}(\bar{\Lambda}_c^-) = \sqrt{(2E_{\rm beam} - E_{\bar{\Lambda}_c^-})^2/c^4 - |\vec{p}_{\bar{\Lambda}_c^-}|^2/c^2}, \quad (2)$$

is required to fall inside the range $(2.275, 2.310)$ GeV$/c^2$, where $E_{\rm beam}$ is the beam energy, and $E_{\bar{\Lambda}_c^-}$ and $\vec{p}_{\bar{\Lambda}_c^-}$ are the energy and momentum of the ST $\bar{\Lambda}_c^-$, respectively. To remove the peaking background due to the process $\Lambda_c^+ \to \Sigma^+ K^+ \pi^-$, we exclude events with $M_{\rm rec}(H^+) \in (1.15, 1.24)$ GeV$/c^2$, where the recoiling mass $M_{\rm rec}(H^+)$ is as defined in Eq. (1), with the subscript i now representing the K^+ and π^- particles. Additionally, to suppress the potential background from $\Lambda_c^+ \to n K_S^0 K^+$ decays, events satisfying $M(\pi^+\pi^-) \in (0.48, 0.52)$ GeV$/c^2$ are vetoed where $M(\pi^+\pi^-)$ is the invariant mass of the $\pi^+\pi^-$ pair. The requirement $M_{\rm rec}(H^-) > 1.15$ GeV$/c^2$ is imposed to suppress backgrounds due to the $q\bar{q}$ and nonsignal $\Lambda_c^+\bar{\Lambda}_c^-$ processes.

The two-dimensional (2D) distribution of $M_{\rm rec}(H^-)$ and $M_{\rm rec}(B^0)$ is shown in Fig. 2(a), where the events containing both a Σ^- and a neutron are clustered close to the left-bottom corner, indicating the existence of the singly CS decay $\Lambda_c^+ \to \Sigma^- K^+ \pi^+$ with $\Sigma^- \to n\pi^-$. A large number of events containing a Λ and Ξ^- appear in the central region of the 2D distribution, which originate from the CF decay $\Lambda_c^+ \to \Xi^- K^+ \pi^-$ with $\Xi^- \to \Lambda\pi^-$ and Λ decaying into neutral particles. These resonances are also observed in the projected distributions of $M_{\rm rec}(B^0)$ and $M_{\rm rec}(H^-)$, as shown in Figs. 2(b) and 2(c), respectively. Furthermore, by selecting the events in the Ξ^- signal region $M_{\rm rec}(H^-) \in (1.294, 1.340)$ GeV$/c^2$, the Ξ^{*0} signal is observed, originating from the process $\Lambda_c^+ \to \Xi^{*0} K^+$ with $\Xi^{*0} \to \Xi^- \pi^+$, in the distribution of $M_{\rm rec}(K^+)$ as shown in Fig. 2(d). Here the variable $M_{\rm rec}(K^+)$ is also determined according to Eq. (1), with the subscript i labeling only the K^+ particle.

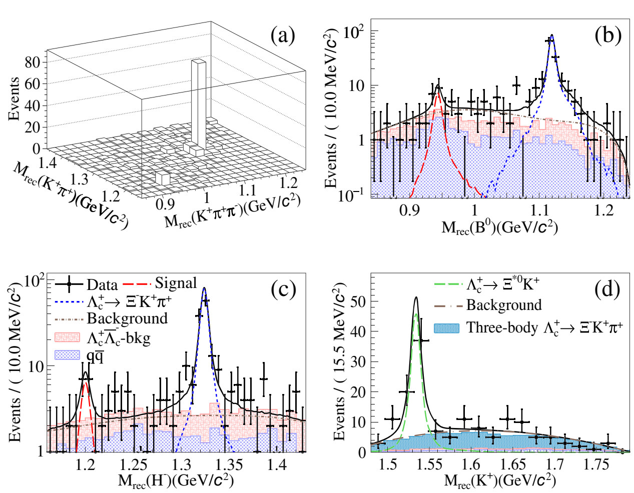

FIG. 2. The 2D distribution of $M_{\rm rec}(K^+\pi^+)$ versus $M_{\rm rec}(K^+\pi^+\pi^-)$ (a), the distributions of $M_{\rm rec}(K^+\pi^+\pi^-)$ (b), $M_{\rm rec}(K^+\pi^+)$ (c), and $M_{\rm rec}(K^+)$ (d) of the accepted DT candidate events from data for all energy points. The black points with error bars are data. The curves represent the fit results, including the signal and background components, respectively.

Potential backgrounds are classified into two categories: $q\bar{q}$ processes, and $e^+e^- \to \Lambda_c^+\bar{\Lambda}_c^-$ events excluding signal contributions of $\Lambda_c^+ \to \Sigma^- K^+ \pi^+$, $\Xi^- K^+ \pi^+$, and $\Xi^{*0} K^+$ (referred to as $\Lambda_c^+\bar{\Lambda}_c^-$ background hereafter). The $q\bar{q}$ and $\Lambda_c^+\bar{\Lambda}_c^-$ backgrounds are investigated with the inclusive MC samples with an integrated luminosity 40 times higher than that of data, and they are normalized to the same integrated luminosity as the data. No peaking background is observed in these samples. In Figs. 2(b) and 2(c), the components of $q\bar{q}$ and $\Lambda_c^+\bar{\Lambda}_c^-$ backgrounds are described with the inclusive MC samples that are normalized with the scale factor 0.034. The scale factor is obtained by comparing the number of events between data and inclusive MC samples in the sideband region $M_{BC} \in (2.10, 2.25)$ GeV$/c^2$ of ST $\bar{\Lambda}_c^-$.

The signal yields ($N_{\rm obs}$) of the $\Lambda_c^+ \to \Sigma^- K^+ \pi^+$ and $\Xi^- K^+ \pi^+$ decays are obtained by performing an unbinned maximum-likelihood fit to the 2D distribution of $M_{\rm rec}(H^-)$ and $M_{\rm rec}(B^0)$, where the 2D signal shapes are modeled by the simulated shapes for the two decays, respectively, convolved with the same Gaussian function accounting for the resolution difference between data and MC simulation. The 2D shape of $q\bar{q}$ and $\Lambda_c^+\bar{\Lambda}_c^-$ backgrounds is modeled with the product of two third-order Chebyshev polynomial functions and a Student distribution [34–37] that is used to describe the dispersion of the backgrounds in the diagonal direction. Details of the background functions and the validation are given in the Supplemental Material [33]. Additionally, a fit to the distribution of $M_{\rm rec}(K^+)$ is performed simultaneously to determine the yield of the decay $\Lambda_c^+ \to \Xi(1530)^0 K^+$, where its shape is also described from the simulation convolved with an individual Gaussian function. Here, the $q\bar{q}$ and $\Lambda_c^+\bar{\Lambda}_c^-$ backgrounds are described individually by two third-order Chebyshev polynomials, whose shape parameters are obtained from fits to the corresponding inclusive MC samples, and whose magnitudes are determined from the fit to the data. In addition, the nonresonant three-body decay $\Lambda_c^+ \to \Xi^- K^+ \pi^+$ has a smooth distribution in $M_{\rm rec}(K^+)$, and is also modeled by a third-order Chebyshev polynomial with its shape parameters obtained from the MC simulation, and its magnitude determined from the fit to data. The yield of $\Lambda_c^+ \to \Xi^- K^+ \pi^+$ decays in the 2D fit is constrained to be equal to the sum of those of the decay $\Lambda_c^+ \to \Xi(1530)^0 K^+$ and the three-body decay $\Lambda_c^+ \to \Xi^- K^+ \pi^+$ in the fit to the distribution of $M_{\rm rec}(K^+)$. The yield of $q\bar{q}$ and $\Lambda_c^+\bar{\Lambda}_c^-$ backgrounds in the region $M_{\rm rec}(H^-) \in (1.294, 1.340)$ GeV$/c^2$ is fixed to the numbers obtained from the fit to the distribution of $M_{\rm rec}(K^+)$. The resultant fit is depicted in Fig. 2, and the signal yields are determined to be 12 ± 4, 128 ± 13, and 54 ± 8 for $\Lambda_c^+ \to \Sigma^- K^+ \pi^+$, $\Xi^- K^+ \pi^+$, and $\Xi^{*0} K^+$, respectively, where the uncertainties are statistical. The statistical significance of the $\Lambda_c^+ \to \Sigma^- K^+ \pi^+$ signal is 5.4σ, which is calculated from the change of the likelihood values between fits with and without the signal component, accounting for the change in the number of degrees of freedom and taking into account both statistical and systematic uncertainties. The details of how to take the systematic uncertainty into account are shown in the Supplemental Material [33].

The branching fractions ($\mathcal{B}$) are determined as

$$\mathcal{B} = \frac{N_{\rm obs}}{\sum_{ij} N_{ij}^{\rm ST} \cdot (\epsilon_{ij}^{\rm DT}/\epsilon_{ij}^{\rm ST})}, \quad (3)$$

where the subscripts i and j label the ST modes and the data samples at individual c.m. energies, respectively. The parameters $N_{ij}^{\rm ST}$, $\epsilon_{ij}^{\rm ST}$, and $\epsilon_{ij}^{\rm DT}$ are the ST yields, and ST and DT efficiencies, respectively. The detection efficiencies $\epsilon_{ij}^{\rm ST}$ and $\epsilon_{ij}^{\rm DT}$ are estimated from signal MC samples, where the key distributions of the ST modes have been reweighted to agree with those of data. Since the decay $\Lambda_c^+ \to \Xi^- K^+ \pi^+$ has two major components, i.e., $\Lambda_c^+ \to \Xi(1530)^0 K^+$ and the nonresonant three-body decay $\Lambda_c^+ \to \Xi^- K^+ \pi^+$, its detection efficiencies combine the contributions from both of these two components. To take into account potential intermediate-resonance effects, the signal MC sample of $\Lambda_c^+ \to \Xi^- K^+ \pi^+$ is reweighted to match the data together with the $\Lambda_c^+ \to \Xi(1530)^0 K^+$ component, and the DT efficiencies of the decay $\Lambda_c^+ \to \Xi^- K^+ \pi^+$ are derived. Details of the weights could be found in the Supplemental Material [33]. The ST efficiencies can be found in Supplemental Material [33], whereas the DT efficiencies are summarized in Table I. The BFs are determined to be $\mathcal{B}(\Lambda_c^+ \to \Sigma^- K^+ \pi^+) = (3.8 \pm 1.2 \pm 0.2) \times 10^{-4}$, $\mathcal{B}(\Lambda_c^+ \to \Xi^- K^+ \pi^+) = (7.74 \pm 0.76 \pm 0.54) \times 10^{-3}$, and $\mathcal{B}(\Lambda_c^+ \to \Xi(1530)^0 K^+) = (5.03 \pm 0.77 \pm 0.20) \times 10^{-3}$, where the first uncertainties are statistical and the second are systematic.

Benefiting from the DT approach, the systematic uncertainties associated with the ST selection efficiency cancel out in the branching-fraction measurements. Thus, the systematic uncertainties for these measurements comprise those associated with the ST yields, the K^+ and $\pi^\pm$ tracking and PID efficiencies, the requirement on the number of tracks, the determination of the DT signal yields, the branching fraction of the intermediate-state decays, and the statistical uncertainties from the signal MC samples.

The uncertainty in the total ST yields is 0.5% [31,32], which arises from the statistical uncertainty and fitting strategy for extracting these yields. The uncertainties associated with the K^+ and $\pi^\pm$ tracking and PID efficiencies are both assigned to be 1.0%, from studies performed with control samples of $J/\psi \to K_S^0 K^\pm \pi^\mp$, $K_S^0 \to \pi^+\pi^-$ [38], and $J/\psi \to \pi^+\pi^-\pi^0$ [39] decays. The uncertainty due to the no extra charged track requirement is 2.2%, which is assigned from studies of a control sample of $e^+e^- \to \Lambda_c^+\bar{\Lambda}_c^-$ decays, with $\Lambda_c^+ \to pK^-\pi^+$ and the $\bar{\Lambda}_c^-$ decaying into the ten tagged decay modes. The uncertainties from the determination of the DT yields are 3.7%, 2.1%, and 2.2% for the decays $\Lambda_c^+ \to \Sigma^- K^+ \pi^+$, $\Xi^- K^+ \pi^+$, and $\Xi^{*0} K^+$, respectively, including those from the modeling of $q\bar{q}$ and $\Lambda_c^+\bar{\Lambda}_c^-$ backgrounds, which are estimated by considering the uncertainty in the scale factor for the $q\bar{q}$ estimation and in the parameters of the Chebyshev polynomial functions and the students distribution for describing the shape of $q\bar{q}$ and $\Lambda_c^+\bar{\Lambda}_c^-$ backgrounds. The uncertainties in the quoted branching fractions of Ξ^- and Ξ^{*0} are both 1.4% for the decays $\Lambda_c^+ \to \Xi^- K^+ \pi^+$ and $\Xi^{*0} K^+$, respectively. The uncertainty arising from the MC modeling for $\Lambda_c^+ \to \Xi^- K^+ \pi^+$ is investigated by reweighting the MC distribution to data, and comparing with the results obtained between the original and reweighted samples. The resultant uncertainty in the MC modeling is 5.9%. The uncertainties associated with the finite size of the signal MC samples are 0.5%. Assuming that all of the sources of bias are uncorrelated, the total uncertainties are then taken to be the quadratic sum of the individual contributions, which are 4.9%, 6.9%, and 4.0% for $\Lambda_c^+ \to \Sigma^- K^+ \pi^+$, $\Xi^- K^+ \pi^+$, and $\Xi^{*0} K^+$, respectively.

In summary, the singly Cabibbo-suppressed decay $\Lambda_c^+ \to \Sigma^- K^+ \pi^+$ is observed for the first time with a statistical significance of 5.4σ by analyzing e^+e^- collision data samples corresponding to a total integrated luminosity of 4.5 fb^{-1} collected at c.m. energies between 4.600 and 4.699 GeV with the BESIII detector. The branching fraction of $\Lambda_c^+ \to \Sigma^- K^+ \pi^+$ is measured to be $(3.8 \pm 1.2_{\rm stat} \pm 0.2_{\rm syst}) \times 10^{-4}$ with a model-independent approach. This is the first observation of the CS Λ_c^+ decay containing a Σ^- in the final state. The ratio of branching fractions between $\Lambda_c^+ \to \Sigma^- K^+ \pi^+$ and the CF decay $\Lambda_c^+ \to \Sigma^-\pi^+\pi^+$ [3] is observed to be $(2.03 \pm 0.73)\% \simeq (0.4 \pm 0.1)s_c^2$, which is close to the ratio $\mathcal{B}(\Xi_c^0 \to \Xi^- K^+)/\mathcal{B}(\Xi_c^0 \to \Xi^- \pi^+)$ and deviates significantly from $1.0 s_c^2$, while $1.0 s_c^2$ is also consistent with CS/CF ratio of the isospin partner modes $\mathcal{B}(\Lambda_c^+ \to \Sigma^+ K^+ \pi^-)/\mathcal{B}(\Lambda_c^+ \to \Sigma^+ \pi^+ \pi^-)$. This result suggests nonfactorization contribution is dominate over the factorization one or large SU(3) flavor symmetry breaking effect in three-body decays involving a Σ^- baryon. A prediction based on $SU(3)_F$ symmetry gave $\mathcal{B}^{\rm pred}(\Lambda_c^+ \to \Sigma^- K^+ \pi^+) = (3.3 \pm 2.3) \times 10^{-4}$ [40], which has a larger uncertainty than our measurement due to the limited sample sizes of the channels used as inputs to the calculation. Our measurement provides direct information to improve the understanding of the Λ_c^+ decay mechanisms. Meanwhile, the branching fractions of CF decays $\Lambda_c^+ \to \Xi^- K^+ \pi^+$ and $\Lambda_c^+ \to \Xi(1530)^0 K^+$ are measured to be $(7.74 \pm 0.76_{\rm stat} \pm 0.54_{\rm syst}) \times 10^{-3}$ and $(5.03 \pm 0.77_{\rm stat} \pm 0.20_{\rm syst}) \times 10^{-3}$, respectively, which are consistent with previous results [3]. The measured $\Lambda_c^+ \to \Xi^- K^+ \pi^+$ is the sum of nonresonant three-body decay and $\Lambda_c^+ \to \Xi(1530)^0 K^+$.

The BESIII collaboration thanks the staff of BEPCII, the IHEP computing center and the supercomputing center of the University of Science and Technology of China (USTC) for their strong support. Authors are grateful to Hai-Yang Cheng, Fanrong Xu, and Yu-Kuo Hsiao for enlightening discussions. This work is supported in part by National Key R&D Program of China under Contracts No. 2020YFA0406400 and No. 2020YFA0406300; National Natural Science Foundation of China (NSFC) under Contracts No. 11335008, No. 11625523, No. 11635010, No. 11735014, No. 11822506, No. 11835012, No. 11935015, No. 11935016, No. 11935018, No. 11961141012, No. 12022510, No. 12025502, No. 12035009, No. 12035013, No. 12061131003, No. 12005311, No. 11805086, No. 11705192, and No. 11950410506; the Fundamental Research Funds for the Central Universities, University of Science and Technology of China, Sun Yat-sen University, Lanzhou University, University of Chinese Academy of Sciences; 100 Talents Program of Sun Yat-sen University; the Chinese Academy of Sciences (CAS) Large-Scale Scientific Facility Program; Joint Large-Scale Scientific Facility Funds of the NSFC and CAS under Contracts No. U1732263, No. U1832207, No. U1832103, and No. U2032111; CAS Key Research Program of Frontier Sciences under Contract No. QYZDJ-SSW-SLH040; 100 Talents Program of CAS; China Postdoctoral Science Foundation under Contracts No. 2019M662152 and No. 2020T130636; The Institute of Nuclear and Particle Physics (INPAC) and Shanghai Key Laboratory for Particle Physics and Cosmology; ERC under Contract No. 758462; European Union Horizon 2020 research and innovation program under Contract No. Marie Sklodowska-Curie Grant Agreement No. 894790; German Research Foundation DFG under Contracts No. 443159800, Collaborative Research Center CRC 1044, FOR 2359, FOR 2359, GRK 214; Istituto Nazionale di Fisica Nucleare, Italy; Ministry of Development of Turkey under Contract No. DPT2006K-120470; National Science and Technology fund; Olle Engkvist Foundation under Contract No. 200-0605; STFC (United Kingdom); The Knut and Alice Wallenberg Foundation (Sweden) under Contract No. 2016.0157; The Royal Society, U.K. under Contracts No. DH140054 and No. DH160214; The Swedish Research Council; and U.S. Department of Energy under Contracts No. DE-FG02-05ER41374 and No. DE-SC-0012069.

[1] Y. Kohara, Phys. Rev. D **44**, 2799 (1991).
[2] C. Q. Geng, Y. K. Hsiao, C. W. Liu, and T. H. Tsai, Eur. Phys. J. C **78**, 593 (2018).
[3] R. L. Workman *et al.* (Particle Data Group), Prog. Theor. Exp. Phys. **2022**, 083C01 (2022).
[4] M. Ablikim *et al.* (BESIII Collaboration), Phys. Rev. D **106**, L111101 (2022).
[5] H. Y. Cheng, X. W. Kang, and F. R. Xu, Phys. Rev. D **97**, 074028 (2018).
[6] C. Q. Geng, Y. K. Hsiao, C. W. Liu, and T. H. Tsai, Phys. Rev. D **97**, 073006 (2018).
[7] C. Q. Geng, C. W. Liu, and T. H. Tsai, Phys. Lett. B **790**, 225 (2019).
[8] H. Y. Cheng, Front. Phys. **10**, 101406 (2015).
[9] H. Y. Cheng, Chin. J. Phys. (Taipei) **78**, 324 (2022).
[10] M. Ablikim *et al.* (BESIII Collaboration), Phys. Rev. Lett. **128**, 142001 (2022).
[11] K. K. Sharma and R. C. Verma, Phys. Rev. D **55**, 7067 (1997).
[12] T. Uppal, R. C. Verma, and M. P. Khanna, Phys. Rev. D **49**, 3417 (1994).
[13] C. D. Lü, W. Wang, and F. S. Yu, Phys. Rev. D **93**, 056008 (2016).
[14] H. J. Zhao, Y. L. Wang, Y. K. Hsiao, and Y. Yu, J. High Energy Phys. 02 (2020) 165.
[15] J. Q. Zou, F. R. Xu, G. B. Meng, and H. Y. Cheng, Phys. Rev. D **101**, 014011 (2020).
[16] M. Ablikim *et al.* (BESIII Collaboration), Phys. Rev. D **108**, L031101 (2023).
[17] M. Ablikim *et al.* (BESIII Collaboration), Phys. Rev. Lett. **117**, 232002 (2016).
[18] R. Aaij *et al.* (LHCb Collaboration), J. High Energy Phys. 03 (2014) 043.
[19] M. Ablikim *et al.* (*BABAR* Collaboration), Phys. Rev. D **75**, 052002 (2007).
[20] K. Abe *et al.* (Belle Collaboration), Phys. Lett. B **524**, 33 (2002).
[21] B. Q. Ke, J. Koponen, H.-B.Li, and Y. Zheng, Annu. Rev. Nucl. Part. Sci. **73**, 285 (2023).
[22] M. Ablikim *et al.* (BESIII Collaboration), Nucl. Instrum. Methods Phys. Res., Sect. A **614**, 345 (2010).

[23] S. Agostinelli et al. (GEANT4 Collaboration), Nucl. Instrum. Methods Phys. Res., Sect. A **506**, 250 (2003).
[24] K. X. Huang et al., Nucl. Sci. Tech. **33**, 142 (2022).
[25] S. Jadach, B. F. L. Ward, and Z. Was, Phys. Rev. D **63**, 113009 (2001).
[26] D. J. Lange, Nucl. Instrum. Methods Phys. Res., Sect. A **462**, 152 (2001).
[27] R. G. Ping, Chin. Phys. C **32**, 599 (2008).
[28] J. C. Chen, G. S. Huang, X. R. Qi, D. H. Zhang, and Y. S. Zhu, Phys. Rev. D **62**, 034003 (2000).
[29] Y. L. Yang, R. G. Ping, and H. Chen, Phys. Rev. Lett. **31**, 061301 (2014).
[30] E. R. Was, Phys. Lett. B **303**, 163 (1993).
[31] M. Ablikim et al. (BESIII Collaboration), Phys. Rev. D **106**, 072002 (2022).
[32] M. Ablikim et al. (BESIII Collaboration), Phys. Rev. D **106**, 072008 (2022).
[33] See Supplemental Material at http://link.aps.org/supplemental/10.1103/PhysRevD.109.L071103 for additional details on the detection efficiencies for the other data samples and the background model for the fit.
[34] *The Concise Encyclopedia of Statistics* (Springer, New York, 2008), ISBN: 978-0-387-31742-7.
[35] T. Peng et al. (Belle Collaboration), Phys. Rev. D **89**, 091103 (2014).
[36] M. Ablikim et al. (BESIII Collaboration), arXiv.2311.06883.
[37] M. Ablikim et al. (BESIII Collaboration), arXiv.2312.02524.
[38] M. Ablikim et al. (BESIII Collaboration), Phys. Rev. D **99**, 012003 (2019).
[39] M. Ablikim et al. (BESIII Collaboration), Phys. Rev. D **96**, 112012 (2017).
[40] C. Q. Geng, Y. K. Hsiao, C. W. Liu, and T. H. Tsai, Phys. Rev. D **99**, 073003 (2019).

Correction: The previously published Fig. 1 contained minor typographical errors and has been replaced.

M. Ablikim,[1] M. N. Achasov,[5,b] P. Adlarson,[74] X. C. Ai,[80] R. Aliberti,[35] A. Amoroso,[73a,73c] M. R. An,[39] Q. An,[70,57] Y. Bai,[56] O. Bakina,[36] I. Balossino,[29a] Y. Ban,[46,g] V. Batozskaya,[1,44] K. Begzsuren,[32] N. Berger,[35] M. Berlowski,[44] M. Bertani,[28a] D. Bettoni,[29a] F. Bianchi,[73a,73c] E. Bianco,[73a,73c] A. Bortone,[73a,73c] I. Boyko,[36] R. A. Briere,[6] A. Brueggemann,[67] H. Cai,[75] X. Cai,[1,57] A. Calcaterra,[28a] G. F. Cao,[1,62] N. Cao,[1,62] S. A. Cetin,[61a] J. F. Chang,[1,57] T. T. Chang,[76] W. L. Chang,[1,62] G. R. Che,[43] G. Chelkov,[36,a] C. Chen,[43] Chao Chen,[54] G. Chen,[1] H. S. Chen,[1,62] M. L. Chen,[1,57,62] S. J. Chen,[42] S. M. Chen,[60] T. Chen,[1,62] X. R. Chen,[31,62] X. T. Chen,[1,62] Y. B. Chen,[1,57] Y. Q. Chen,[34] Z. J. Chen,[25,h] W. S. Cheng,[73c] S. K. Choi,[11] X. Chu,[43] G. Cibinetto,[29a] S. C. Coen,[4] F. Cossio,[73c] J. J. Cui,[49] H. L. Dai,[1,57] J. P. Dai,[78] A. Dbeyssi,[18] R. E. de Boer,[4] D. Dedovich,[36] Z. Y. Deng,[1] A. Denig,[35] I. Denysenko,[36] M. Destefanis,[73a,73c] F. De Mori,[73a,73c] B. Ding,[65,1] X. X. Ding,[46,g] Y. Ding,[40] Y. Ding,[34] J. Dong,[1,57] L. Y. Dong,[1,62] M. Y. Dong,[1,57,62] X. Dong,[75] M. C. Du,[1] S. X. Du,[80] Z. H. Duan,[42] P. Egorov,[36,a] Y. H. Y. Fan,[45] Y. L. Fan,[75] J. Fang,[1,57] S. S. Fang,[1,62] W. X. Fang,[1] Y. Fang,[1] R. Farinelli,[29a] L. Fava,[73b,73c] F. Feldbauer,[4] G. Felici,[28a] C. Q. Feng,[70,57] J. H. Feng,[58] K. Fischer,[68] M. Fritsch,[4] C. Fritzsch,[67] C. D. Fu,[1] J. L. Fu,[62] Y. W. Fu,[1] H. Gao,[62] Y. N. Gao,[46,g] Yang Gao,[70,57] S. Garbolino,[73c] I. Garzia,[29a,29b] P. T. Ge,[75] Z. W. Ge,[42] C. Geng,[58] E. M. Gersabeck,[66] A. Gilman,[68] K. Goetzen,[14] L. Gong,[40] W. X. Gong,[1,57] W. Gradl,[35] S. Gramigna,[29a,29b] M. Greco,[73a,73c] M. H. Gu,[1,57] C. Y. Guan,[1,62] Z. L. Guan,[22] A. Q. Guo,[31,62] L. B. Guo,[41] M. J. Guo,[49] R. P. Guo,[48] Y. P. Guo,[13,f] A. Guskov,[36,a] T. T. Han,[49] W. Y. Han,[39] X. Q. Hao,[19] F. A. Harris,[64] K. K. He,[54] K. L. He,[1,62] F. H. H. Heinsius,[4] C. H. Heinz,[35] Y. K. Heng,[1,57,62] C. Herold,[59] T. Holtmann,[4] P. C. Hong,[13,f] G. Y. Hou,[1,62] X. T. Hou,[1,62] Y. R. Hou,[62] Z. L. Hou,[1] H. M. Hu,[1,62] J. F. Hu,[55,i] T. Hu,[1,57,62] Y. Hu,[1] G. S. Huang,[70,57] K. X. Huang,[58] L. Q. Huang,[31,62] X. T. Huang,[49] Y. P. Huang,[1] T. Hussain,[72] N. Hüsken,[27,35] W. Imoehl,[27] J. Jackson,[27] S. Jaeger,[4] S. Janchiv,[32] J. H. Jeong,[11] Q. Ji,[1] Q. P. Ji,[19] X. B. Ji,[1,62] X. L. Ji,[1,57] Y. Y. Ji,[49] X. Q. Jia,[49] Z. K. Jia,[70,57] H. J. Jiang,[75] P. C. Jiang,[46,g] S. S. Jiang,[39] T. J. Jiang,[16] X. S. Jiang,[1,57,62] Y. Jiang,[62] J. B. Jiao,[49] Z. Jiao,[23] S. Jin,[42] Y. Jin,[65] M. Q. Jing,[1,62] T. Johansson,[74] X. K.,[1] S. Kabana,[33] N. Kalantar-Nayestanaki,[63] X. L. Kang,[10] X. S. Kang,[40] M. Kavatsyuk,[63] B. C. Ke,[80] A. Khoukaz,[67] R. Kiuchi,[1] R. Kliemt,[14] O. B. Kolcu,[61a] B. Kopf,[4] M. Kuessner,[4] A. Kupsc,[44,74] W. Kühn,[37] J. J. Lane,[66] P. Larin,[18] A. Lavania,[26] L. Lavezzi,[73a,73c] T. T. Lei,[70,57] Z. H. Lei,[70,57] H. Leithoff,[35] M. Lellmann,[35] T. Lenz,[35] C. Li,[43] C. Li,[47] C. H. Li,[39] Cheng Li,[70,57] D. M. Li,[80] F. Li,[1,57] G. Li,[1] H. Li,[70,57] H. B. Li,[1,62] H. J. Li,[19] H. N. Li,[55,i] Hui Li,[43] J. R. Li,[60] J. S. Li,[58] J. W. Li,[49] K. L. Li,[19] Ke Li,[1] L. J. Li,[1,62] L. K. Li,[1] Lei Li,[3] M. H. Li,[43] P. R. Li,[38,j,k] Q. X. Li,[49] S. X. Li,[13] T. Li,[49] W. D. Li,[1,62] W. G. Li,[1] X. H. Li,[70,57] X. L. Li,[49] Xiaoyu Li,[1,62] Y. G. Li,[46,g] Z. J. Li,[58] C. Liang,[42] H. Liang,[70,57] H. Liang,[34] H. Liang,[1,62] Y. F. Liang,[53] Y. T. Liang,[31,62] G. R. Liao,[15] L. Z. Liao,[49] Y. P. Liao,[1,62] J. Libby,[26] A. Limphirat,[59] D. X. Lin,[31,62] T. Lin,[1] B. J. Liu,[1] B. X. Liu,[75] C. Liu,[34] C. X. Liu,[1] F. H. Liu,[52] Fang Liu,[1] Feng Liu,[7] G. M. Liu,[55,i] H. Liu,[38,j,k] H. M. Liu,[1,62] Huanhuan Liu,[1] Huihui Liu,[21] J. B. Liu,[70,57] J. L. Liu,[71] J. Y. Liu,[1,62] K. Liu,[1] K. Y. Liu,[40] Ke Liu,[22] L. Liu,[70,57] L. C. Liu,[43] Lu Liu,[43] M. H. Liu,[13,f] P. L. Liu,[1] Q. Liu,[62] S. B. Liu,[70,57] T. Liu,[13,f] W. K. Liu,[43] W. M. Liu,[70,57] X. Liu,[38,j,k] Y. Liu,[38,j,k] Y. Liu,[80] Y. B. Liu,[43] Z. A. Liu,[1,57,62] Z. Q. Liu,[49] X. C. Lou,[1,57,62] F. X. Lu,[58] H. J. Lu,[23] J. G. Lu,[1,57] X. L. Lu,[1] Y. Lu,[8] Y. P. Lu,[1,57]

Z. H. Lu,[1,62] C. L. Luo,[41] M. X. Luo,[79] T. Luo,[13,f] X. L. Luo,[1,57] X. R. Lyu,[62] Y. F. Lyu,[43] F. C. Ma,[40] H. L. Ma,[1] J. L. Ma,[1,62] L. L. Ma,[49] M. M. Ma,[1,62] Q. M. Ma,[1] R. Q. Ma,[1,62] R. T. Ma,[62] X. Y. Ma,[1,57] Y. Ma,[46,g] Y. M. Ma,[31] F. E. Maas,[18] M. Maggiora,[73a,73c] S. Malde,[68] Q. A. Malik,[72] A. Mangoni,[28b] Y. J. Mao,[46,g] Z. P. Mao,[1] S. Marcello,[73a,73c] Z. X. Meng,[65] J. G. Messchendorp,[14,63] G. Mezzadri,[29a] H. Miao,[1,62] T. J. Min,[42] R. E. Mitchell,[27] X. H. Mo,[1,57,62] N. Yu. Muchnoi,[5,b] J. Muskalla,[35] Y. Nefedov,[36] F. Nerling,[18,d] I. B. Nikolaev,[5,b] Z. Ning,[1,57] S. Nisar,[12,l] W. D. Niu,[54] Y. Niu,[49] S. L. Olsen,[62] Q. Ouyang,[1,57,62] S. Pacetti,[28b,28c] X. Pan,[54] Y. Pan,[56] A. Pathak,[34] P. Patteri,[28a] Y. P. Pei,[70,57] M. Pelizaeus,[4] H. P. Peng,[70,57] K. Peters,[14,d] J. L. Ping,[41] R. G. Ping,[1,62] S. Plura,[35] S. Pogodin,[36] V. Prasad,[33] F. Z. Qi,[1] H. Qi,[70,57] H. R. Qi,[60] M. Qi,[42] T. Y. Qi,[13,f] S. Qian,[1,57] W. B. Qian,[62] C. F. Qiao,[62] J. J. Qin,[71] L. Q. Qin,[15] X. P. Qin,[13,f] X. S. Qin,[49] Z. H. Qin,[1,57] J. F. Qiu,[1] S. Q. Qu,[60] C. F. Redmer,[35] K. J. Ren,[39] A. Rivetti,[73c] M. Rolo,[73c] G. Rong,[1,62] Ch. Rosner,[18] S. N. Ruan,[43] N. Salone,[44] A. Sarantsev,[36,c] Y. Schelhaas,[35] K. Schoenning,[74] M. Scodeggio,[29a,29b] K. Y. Shan,[13,f] W. Shan,[24] X. Y. Shan,[70,57] J. F. Shangguan,[54] L. G. Shao,[1,62] M. Shao,[70,57] C. P. Shen,[13,f] H. F. Shen,[1,62] W. H. Shen,[62] X. Y. Shen,[1,62] B. A. Shi,[62] H. C. Shi,[70,57] J. L. Shi,[13] J. Y. Shi,[1] Q. Q. Shi,[54] R. S. Shi,[1,62] X. Shi,[1,57] J. J. Song,[19] T. Z. Song,[58] W. M. Song,[34,1] Y. J. Song,[13] Y. X. Song,[46,g] S. Sosio,[73a,73c] S. Spataro,[73a,73c] F. Stieler,[35] Y. J. Su,[62] G. B. Sun,[75] G. X. Sun,[1] H. Sun,[62] H. K. Sun,[1] J. F. Sun,[19] K. Sun,[60] L. Sun,[75] S. S. Sun,[1,62] T. Sun,[1,62] W. Y. Sun,[34] Y. Sun,[10] Y. J. Sun,[70,57] Y. Z. Sun,[1] Z. T. Sun,[49] Y. X. Tan,[70,57] C. J. Tang,[53] G. Y. Tang,[1] J. Tang,[58] Y. A. Tang,[75] L. Y. Tao,[71] Q. T. Tao,[25,h] M. Tat,[68] J. X. Teng,[70,57] V. Thoren,[74] W. H. Tian,[51] W. H. Tian,[58] Y. Tian,[31,62] Z. F. Tian,[75] I. Uman,[61b] S. J. Wang,[49] B. Wang,[1] B. L. Wang,[62] Bo Wang,[70,57] C. W. Wang,[42] D. Y. Wang,[46,g] F. Wang,[71] H. J. Wang,[38,j,k] H. P. Wang,[1,62] J. P. Wang,[49] K. Wang,[1,57] L. L. Wang,[1] M. Wang,[49] Meng Wang,[1,62] S. Wang,[13,f] S. Wang,[38,j,k] T. Wang,[13,f] T. J. Wang,[43] W. Wang,[58] W. Wang,[71] W. P. Wang,[70,57] X. Wang,[46,g] X. F. Wang,[38,j,k] X. J. Wang,[39] X. L. Wang,[13,f] Y. Wang,[60] Y. D. Wang,[45] Y. F. Wang,[1,57,62] Y. H. Wang,[47] Y. N. Wang,[45] Y. Q. Wang,[1] Yaqian Wang,[17,1] Yi Wang,[60] Z. Wang,[1,57] Z. L. Wang,[71] Z. Y. Wang,[1,62] Ziyi Wang,[62] D. Wei,[69] D. H. Wei,[15] F. Weidner,[67] S. P. Wen,[1] C. W. Wenzel,[4] U. Wiedner,[4] G. Wilkinson,[68] M. Wolke,[74] L. Wollenberg,[4] C. Wu,[39] J. F. Wu,[1,62] L. H. Wu,[1] L. J. Wu,[1,62] X. Wu,[13,f] X. H. Wu,[34] Y. Wu,[70] Y. H. Wu,[54] Y. J. Wu,[31] Z. Wu,[1,57] L. Xia,[70,57] X. M. Xian,[39] T. Xiang,[46,g] D. Xiao,[38,j,k] G. Y. Xiao,[42] S. Y. Xiao,[1] Y. L. Xiao,[13,f] Z. J. Xiao,[41] C. Xie,[42] X. H. Xie,[46,g] Y. Xie,[49] Y. G. Xie,[1,57] Y. H. Xie,[7] Z. P. Xie,[70,57] T. Y. Xing,[1,62] C. F. Xu,[1,62] C. J. Xu,[58] G. F. Xu,[1] H. Y. Xu,[65] Q. J. Xu,[16] Q. N. Xu,[30] W. Xu,[1,62] W. L. Xu,[65] X. P. Xu,[54] Y. C. Xu,[77] Z. P. Xu,[42] Z. S. Xu,[62] F. Yan,[13,f] L. Yan,[13,f] W. B. Yan,[70,57] W. C. Yan,[80] X. Q. Yan,[1] H. J. Yang,[50,e] H. L. Yang,[34] H. X. Yang,[1] Tao Yang,[1] Y. Yang,[13,f] Y. F. Yang,[43] Y. X. Yang,[1,62] Yifan Yang,[1,62] Z. W. Yang,[38,j,k] Z. P. Yao,[49] M. Ye,[1,57] M. H. Ye,[9] J. H. Yin,[1] Z. Y. You,[58] B. X. Yu,[1,57,62] C. X. Yu,[43] G. Yu,[1,62] J. S. Yu,[25,h] T. Yu,[71] X. D. Yu,[46,g] C. Z. Yuan,[1,62] L. Yuan,[2] S. C. Yuan,[1] X. Q. Yuan,[1] Y. Yuan,[1,62] Z. Y. Yuan,[58] C. X. Yue,[39] A. A. Zafar,[72] F. R. Zeng,[49] X. Zeng,[13,f] Y. Zeng,[25,h] Y. J. Zeng,[1,62] X. Y. Zhai,[34] Y. C. Zhai,[49] Y. H. Zhan,[58] A. Q. Zhang,[1,62] B. L. Zhang,[1,62] B. X. Zhang,[1] D. H. Zhang,[43] G. Y. Zhang,[19] H. Zhang,[70] H. H. Zhang,[34] H. H. Zhang,[58] H. Q. Zhang,[1,57,62] H. Y. Zhang,[1,57] J. Zhang,[80] J. J. Zhang,[51] J. L. Zhang,[20] J. Q. Zhang,[41] J. W. Zhang,[1,57,62] J. X. Zhang,[38,j,k] J. Y. Zhang,[1] J. Z. Zhang,[1,62] Jianyu Zhang,[62] Jiawei Zhang,[1,62] L. M. Zhang,[60] L. Q. Zhang,[58] Lei Zhang,[42] P. Zhang,[1,62] Q. Y. Zhang,[39,80] Shuihan Zhang,[1,62] Shulei Zhang,[25,h] X. D. Zhang,[45] X. M. Zhang,[1] X. Y. Zhang,[49] Xuyan Zhang,[54] Y. Zhang,[71] Y. Zhang,[68] Y. T. Zhang,[80] Y. H. Zhang,[1,57] Yan Zhang,[70,57] Yao Zhang,[1] Z. H. Zhang,[1] Z. L. Zhang,[34] Z. Y. Zhang,[43] Z. Y. Zhang,[75] G. Zhao,[1] J. Zhao,[39] J. Y. Zhao,[1,62] J. Z. Zhao,[1,57] Lei Zhao,[70,57] Ling Zhao,[1] M. G. Zhao,[43] S. J. Zhao,[80] Y. B. Zhao,[1,57] Y. X. Zhao,[31,62] Z. G. Zhao,[70,57] A. Zhemchugov,[36,a] B. Zheng,[71] J. P. Zheng,[1,57] W. J. Zheng,[1,62] Y. H. Zheng,[62] B. Zhong,[41] X. Zhong,[58] H. Zhou,[49] L. P. Zhou,[1,62] X. Zhou,[75] X. K. Zhou,[7] X. R. Zhou,[70,57] X. Y. Zhou,[39] Y. Z. Zhou,[13,f] J. Zhu,[43] K. Zhu,[1] K. J. Zhu,[1,57,62] L. Zhu,[34] L. X. Zhu,[62] S. H. Zhu,[69] S. Q. Zhu,[42] T. J. Zhu,[13,f] W. J. Zhu,[13,f] Y. C. Zhu,[70,57] Z. A. Zhu,[1,62] J. H. Zou,[1] and J. Zu[70,57]

(BESIII Collaboration)

[1] *Institute of High Energy Physics, Beijing 100049, People's Republic of China*
[2] *Beihang University, Beijing 100191, People's Republic of China*
[3] *Beijing Institute of Petrochemical Technology, Beijing 102617, People's Republic of China*
[4] *Bochum Ruhr-University, D-44780 Bochum, Germany*
[5] *Budker Institute of Nuclear Physics SB RAS (BINP), Novosibirsk 630090, Russia*
[6] *Carnegie Mellon University, Pittsburgh, Pennsylvania 15213, USA*
[7] *Central China Normal University, Wuhan 430079, People's Republic of China*
[8] *Central South University, Changsha 410083, People's Republic of China*
[9] *China Center of Advanced Science and Technology, Beijing 100190, People's Republic of China*

[10]China University of Geosciences, Wuhan 430074, People's Republic of China
[11]Chung-Ang University, Seoul, 06974, Republic of Korea
[12]COMSATS University Islamabad, Lahore Campus, Defence Road, Off Raiwind Road, 54000 Lahore, Pakistan
[13]Fudan University, Shanghai 200433, People's Republic of China
[14]GSI Helmholtzcentre for Heavy Ion Research GmbH, D-64291 Darmstadt, Germany
[15]Guangxi Normal University, Guilin 541004, People's Republic of China
[16]Hangzhou Normal University, Hangzhou 310036, People's Republic of China
[17]Hebei University, Baoding 071002, People's Republic of China
[18]Helmholtz Institute Mainz, Staudinger Weg 18, D-55099 Mainz, Germany
[19]Henan Normal University, Xinxiang 453007, People's Republic of China
[20]Henan University, Kaifeng 475004, People's Republic of China
[21]Henan University of Science and Technology, Luoyang 471003, People's Republic of China
[22]Henan University of Technology, Zhengzhou 450001, People's Republic of China
[23]Huangshan College, Huangshan 245000, People's Republic of China
[24]Hunan Normal University, Changsha 410081, People's Republic of China
[25]Hunan University, Changsha 410082, People's Republic of China
[26]Indian Institute of Technology Madras, Chennai 600036, India
[27]Indiana University, Bloomington, Indiana 47405, USA
[28a]INFN Laboratori Nazionali di Frascati, I-00044, Frascati, Italy
[28b]INFN Sezione di Perugia, I-06100, Perugia, Italy
[28c]University of Perugia, I-06100, Perugia, Italy
[29a]INFN Sezione di Ferrara, I-44122, Ferrara, Italy
[29b]University of Ferrara, I-44122, Ferrara, Italy
[30]Inner Mongolia University, Hohhot 010021, People's Republic of China
[31]Institute of Modern Physics, Lanzhou 730000, People's Republic of China
[32]Institute of Physics and Technology, Peace Avenue 54B, Ulaanbaatar 13330, Mongolia
[33]Instituto de Alta Investigación, Universidad de Tarapacá, Casilla 7D, Arica 1000000, Chile
[34]Jilin University, Changchun 130012, People's Republic of China
[35]Johannes Gutenberg University of Mainz, Johann-Joachim-Becher-Weg 45, D-55099 Mainz, Germany
[36]Joint Institute for Nuclear Research, 141980 Dubna, Moscow region, Russia
[37]Justus-Liebig-Universitaet Giessen, II. Physikalisches Institut, Heinrich-Buff-Ring 16, D-35392 Giessen, Germany
[38]Lanzhou University, Lanzhou 730000, People's Republic of China
[39]Liaoning Normal University, Dalian 116029, People's Republic of China
[40]Liaoning University, Shenyang 110036, People's Republic of China
[41]Nanjing Normal University, Nanjing 210023, People's Republic of China
[42]Nanjing University, Nanjing 210093, People's Republic of China
[43]Nankai University, Tianjin 300071, People's Republic of China
[44]National Centre for Nuclear Research, Warsaw 02-093, Poland
[45]North China Electric Power University, Beijing 102206, People's Republic of China
[46]Peking University, Beijing 100871, People's Republic of China
[47]Qufu Normal University, Qufu 273165, People's Republic of China
[48]Shandong Normal University, Jinan 250014, People's Republic of China
[49]Shandong University, Jinan 250100, People's Republic of China
[50]Shanghai Jiao Tong University, Shanghai 200240, People's Republic of China
[51]Shanxi Normal University, Linfen 041004, People's Republic of China
[52]Shanxi University, Taiyuan 030006, People's Republic of China
[53]Sichuan University, Chengdu 610064, People's Republic of China
[54]Soochow University, Suzhou 215006, People's Republic of China
[55]South China Normal University, Guangzhou 510006, People's Republic of China
[56]Southeast University, Nanjing 211100, People's Republic of China
[57]State Key Laboratory of Particle Detection and Electronics, Beijing 100049, Hefei 230026, People's Republic of China
[58]Sun Yat-Sen University, Guangzhou 510275, People's Republic of China
[59]Suranaree University of Technology, University Avenue 111, Nakhon Ratchasima 30000, Thailand
[60]Tsinghua University, Beijing 100084, People's Republic of China
[61a]Turkish Accelerator Center Particle Factory Group, Istinye University, 34010, Istanbul, Turkey
[61b]Near East University, Nicosia, North Cyprus, 99138, Mersin 10, Turkey
[62]University of Chinese Academy of Sciences, Beijing 100049, People's Republic of China

[63]University of Groningen, NL-9747 AA Groningen, The Netherlands
[64]University of Hawaii, Honolulu, Hawaii 96822, USA
[65]University of Jinan, Jinan 250022, People's Republic of China
[66]University of Manchester, Oxford Road, Manchester, M13 9PL, United Kingdom
[67]University of Muenster, Wilhelm-Klemm-Strasse 9, 48149 Muenster, Germany
[68]University of Oxford, Keble Road, Oxford OX13RH, United Kingdom
[69]University of Science and Technology Liaoning, Anshan 114051, People's Republic of China
[70]University of Science and Technology of China, Hefei 230026, People's Republic of China
[71]University of South China, Hengyang 421001, People's Republic of China
[72]University of the Punjab, Lahore-54590, Pakistan
[73a]University of Turin and INFN, University of Turin, I-10125, Turin, Italy
[73b]University of Eastern Piedmont, I-15121, Alessandria, Italy
[73c]INFN, I-10125, Turin, Italy
[74]Uppsala University, Box 516, SE-75120 Uppsala, Sweden
[75]Wuhan University, Wuhan 430072, People's Republic of China
[76]Xinyang Normal University, Xinyang 464000, People's Republic of China
[77]Yantai University, Yantai 264005, People's Republic of China
[78]Yunnan University, Kunming 650500, People's Republic of China
[79]Zhejiang University, Hangzhou 310027, People's Republic of China
[80]Zhengzhou University, Zhengzhou 450001, People's Republic of China

[a]Also at the Moscow Institute of Physics and Technology, Moscow 141700, Russia.
[b]Also at the Novosibirsk State University, Novosibirsk, 630090, Russia.
[c]Also at the NRC "Kurchatov Institute," PNPI, 188300, Gatchina, Russia.
[d]Also at Goethe University Frankfurt, 60323 Frankfurt am Main, Germany.
[e]Also at Key Laboratory for Particle Physics, Astrophysics and Cosmology, Ministry of Education; Shanghai Key Laboratory for Particle Physics and Cosmology; Institute of Nuclear and Particle Physics, Shanghai 200240, People's Republic of China.
[f]Also at Key Laboratory of Nuclear Physics and Ion-beam Application (MOE) and Institute of Modern Physics, Fudan University, Shanghai 200443, People's Republic of China.
[g]Also at State Key Laboratory of Nuclear Physics and Technology, Peking University, Beijing 100871, People's Republic of China.
[h]Also at School of Physics and Electronics, Hunan University, Changsha 410082, China.
[i]Also at Guangdong Provincial Key Laboratory of Nuclear Science, Institute of Quantum Matter, South China Normal University, Guangzhou 510006, China.
[j]Also at Frontiers Science Center for Rare Isotopes, Lanzhou University, Lanzhou 730000, People's Republic of China.
[k]Also at Lanzhou Center for Theoretical Physics, Lanzhou University, Lanzhou 730000, People's Republic of China.
[l]Also at the Department of Mathematical Sciences, IBA, Karachi 75270, Pakistan.